

# Towards future spaceborne radar ice and mixed-phase retrievals

S. Nesbitt<sup>1</sup>, P. Borque<sup>1</sup>, R. Chase<sup>1</sup>, J. Finlon<sup>1</sup>, and G. McFarquhar<sup>2</sup>

<sup>1</sup>Department of Atmospheric Sciences, University of Illinois at Urbana-Champaign  
<sup>2</sup>CIMMS, School of Meteorology, University of Oklahoma



## USING GPM FIELD CAMPAIGN OBSERVATIONS FOR IMPROVED RETRIEVALS

The current Global Precipitation Measurement (GPM) Mission Dual-Frequency Precipitation Radar (DPR) algorithm, described in Iguchi et al. (2010) – and subsequently updated for Vo5 – contains a number of models, parameterizations, and other *a priori* assumptions of precipitation in order to relate the satellite observed KuPR and KaPR measured equivalent radar reflectivity factor (Z). Figure 1 summarizes the “building blocks” of the current DPR algorithm, containing several algorithm components that enable the ultimate retrieval of precipitation rate R from the observed values of Z at each frequency. Indeed, generic retrievals using single, dual, or triple frequency algorithms could be developed with these basic components. Of course, the assumptions that go into these components can have drastic impacts on the ultimately retrieved values of R and total water content (TWC).

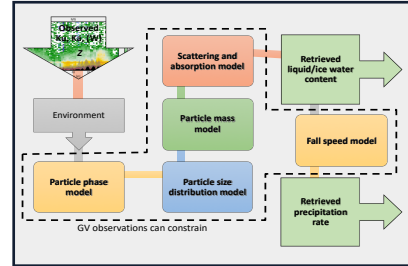


Fig. 1: Retrieval components necessary for a spaceborne radar retrieval. Observations and environmental data are input into models that describe the physical properties of the hydrometeors and their interaction with the radar's scattered energy. Reducing the uncertainty in each of these components of the retrieval algorithm is critical and can be constrained by GPM GV observations.

## AIM

In ice- and mixed-phase precipitation, the uncertainty in each component of a precipitation retrieval algorithm is not well constrained at present. This is contributed to by both the natural variability of ice particles, habits, their PSDs and scattering and absorption properties, but also historically by a relative lack of collocated physical measurements of the properties of these clouds that can yield information on how the “building blocks” of a retrieval should be constrained by observations.

Here we summarize three articles that have used GPM GV observations to address key algorithm components, towards improved spaceborne radar retrieval of ice and mixed-phase precipitation.

## ACKNOWLEDGEMENTS

Funding for this research has been provided by the PMM Science Team and the NESSF Fellowship program to Randy Chase.



## UNCORRELATED MASS PARAMETERS IN ICE CLOUDS

In both dual-frequency and dual-polarization active remote sensing applications, the number of independent observations (2) does not allow constraint of the number of free parameters in a Gamma-style particle size distribution (PSD) model (3). Following the work of Williams et al. (2014) uncorrelated mass parameters can be used to avoid statistical artifacts while developing a relation that allows parameterization of the Gamma shape parameter  $\mu$  based on the PSD bulk property mass-weighted mean diameter ( $D_{mw}$ ).

→ Our recent work (Borque et al. 2018, *JAMC*, in review) extends both the normalized Gamma framework described above and the Williams et al. (2014) mathematical framework for the parameterization of Gamma shape parameter  $\mu$  to ice particles of variable effective density through inclusion of parameters in a mass-dimensional relationship (i.e.,  $m(D) = aD^b$ ). Using this technique, we developed a new parameterization for ice phase PSD observed using observations during the GPM Cold-season Precipitation Experiment (GCPEX), and compare the GCPEX observations with existing PSD parameterizations used in GPM and CloudSat algorithms (Field et al. 2007).

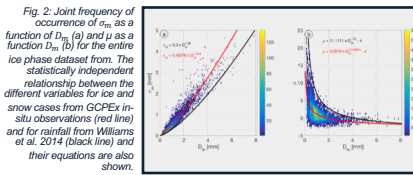


Fig. 2: Joint frequency of occurrence of  $\sigma_m$  as a function of  $D_{mw}$  (a) and  $\mu$  as a function of  $D_{mw}$  (b) for the entire ice phase dataset from the statistically independent relationship between the different variables for ice and snow cases from GCPEX in-situ observations (red line) and for rainfall from Williams et al. 2014 (black line) and their equations are also shown.

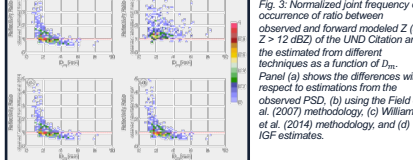


Fig. 3: Normalized joint frequency of occurrence of ratio between observed and forward modeled Z (at  $Z > 12$  dBZ) of the UND Citation and the estimated from different techniques as a function of  $D_{mw}$ . Panel (a) shows the differences with respect to estimations from the observed PSD, (b) using the Field et al. (2007) methodology, (c) Williams et al. (2014) methodology, and (d) IGF estimates.

- Using our new PSD parameterization, we compared forward computed IWC and Rayleigh-regime Z against observed values from the aircraft and C-Band radar reflectivity observations matched to the aircraft position from the ECCC King City radar, respectively.
- For each of these comparisons, our new parameterization produced computed estimates of IWC and Z within 1-3% of those from the actual PSD
- Biases relative to observed IWC and Z (which require the use of a mass-dimension relationship) were also comparable amongst the results from the PSD and the IGF fit, within 10% of the observed values for all observed PSDs.
- Surprisingly, the Field et al. (2007) parameterization used in the CloudSat retrieval performed quite unfavorably compared with the other techniques evaluated, with that PSD formulation leading to a 27% and 45% overestimate in IWC and Z respectively for GPM-detectable PSDs (calculated  $Z > 12$  dBZ).

This work demonstrates that PSD parameterizations can be developed which can be readily tested and used in GPM algorithms, and their uncertainties be examined. The impacts of these improved parameterizations can extend well beyond radar and passive microwave retrievals into other applications such as cloud resolving models; extending this work into other regimes through the use of the GPM field campaign observation database is a critical step in improving GPM retrievals.

## MULTI-FREQUENCY RADAR AND IN SITU OBSERVATIONS IN OLYMPLEX

The GPM GV Olympic Mountains Experiment (OLYMPEX) dataset is unique in that it was the first campaign to collect coincident airborne observations including state parameters, bulk liquid and ice water content, PSD and triple-frequency radar (at Ku-, Ka- and W-band) measurements. Chase et al. (2018, *GRL*) explores the observed parameter space of triple frequency radar observations alongside microphysical observations from the UND Citation aircraft. This dataset can be used to constrain dual-frequency retrievals with applicability to GPM, as well as Ka-W and triple-frequency retrievals of ice and snow, which has been put forth as a potential observational platform for the next generation of spaceborne active sensors.

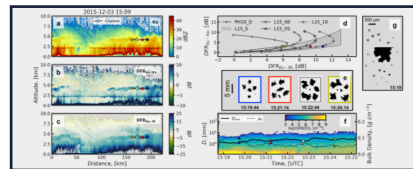


Figure 4: Vertical cross section of (a) Ku-band reflectivity, (b)  $DFR_{Ku-Ka}$ , (c)  $DFR_{Ka-W}$  measured by the APR-3, with UND Citation track overlaid with a colored marker every 90 s corresponding to colors in other subplots. (d) DFR plane containing scattering model curves of a dendrite aggregate (PH10\_D) adapted from Petty and Huang (2010), dendrite aggregates with 0, 0.5 and 1 kg m<sup>-2</sup> of rime ice (L15\_00, L15\_05, and L15\_10 respectively) adapted from Leinonen and Szymer (2015), and 90% of spheroidal approximation for aggregates (L15\_S, black shaded) adapted from Leinonen and Szymer (2015). The polygon is the inferred region where both complex and simple scattering models exist. Colored points are 10 s means of matched DFR values at markers in Figure 2a-c (e) Randomly selected HVPS3 particle images corresponding to the color-times from Figure 2d (f) (ND) (shading).  $D_{mw}$  (solid circles) and  $\rho_e$  (dotted triangles) along the flight track of the Citation in Fig. 2a-c (g) Sample 2DS images from 15:19, showing numerous out of focus spherical particles, inferred to be supercooled drizzle drops.

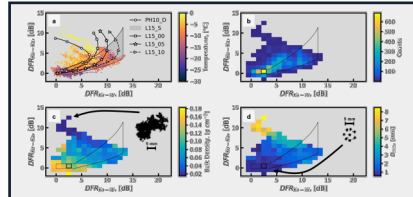


Fig. 5: DFR plane using all 15 matched stratiform flight legs. (a) Scatterplot of all matched instances between the APR-3 and the Citation colored by observed temperature. Curves and polygon are the same as in Fig. 4d. (b) Joint frequency of occurrence of  $DFR_{Ku-Ka}$  vs.  $DFR_{Ka-W}$ , most frequent bin outlined in black. The polygon outlines the region where particle shape is ambiguous. (c) Using the identical 2-D histogram in Fig. 5b but bins are colored by the mean  $\rho_e$  within the bin. An example particle image from the HVPS3 at the indicated region on the DFR plane. (d) As in Fig. 5c but colored by mean  $D_{mw}$  in each bin.

These results support the retrieval of  $D_{mw}$  and  $\rho_e$  using triple-frequency radar observations. Information on these key bulk microphysical parameters are included in the  $DFR_{Ku-Ka}$  and  $DFR_{Ka-W}$ , with more information regarding  $D_{mw}$  and  $\rho_e$  linked to  $DFR_{Ku-Ka}$ . Since the GPM mission collects  $DFR_{Ku-Ka}$ , there is potential for developing improved ice- and mixed-phase retrievals for the GPM mission as well as for current and future multi-frequency ground- and satellite-based multi-frequency radar measurements.

## CONSTRAINING MASS IN ICE CLOUDS USING IN SITU DATA AND RADAR REFLECTIVITY AS INDEPENDENT MEASURES

Accurate assumptions of particle mass in retrieval algorithms is critical for reducing uncertainties in IWC and R in GPM retrievals. Using MC3E and OLYMPEX data, and following Hogan et al. (2012), we have found that no single choice of  $a$  and  $b$  can accurately forward calculate both Z and IWC from the same PSD across hydrometeor types and environments.

In addition, we find that IWC directly measured by the Nevzorov probe tends to be less (up to 50%) than those estimated from the PSD using published mass-diameter relationships. Is this apparent underestimate in IWC for larger particle sizes due to shattering artifacts of the probe (Korolev et al. 2013; Wang et al. 2015)? Or is it driven by changes in values of  $a$  and  $b$  in low density large aggregates? This important question motivates investigating this apparent conundrum to attempt to find methods to reduce particle mass uncertainties for retrievals.

→ We have developed a technique that uses both fields to derive the best  $a$  and  $b$  parameters, yielding a surface representing equally realizable values for  $a$  and  $b$  in the  $a - b$  parameter space (Finlon et al. 2018, *ACP*, in review). Our technique finds values of  $a$  and  $b$  that minimize the  $\chi^2$  difference between the measured IWC and collocated Z observations from ground based or aircraft radars (at Rayleigh wavelengths) and those derived from the PSDs. We define surfaces in  $a/b$  phase space of equally realizable solutions that are within some predefined threshold, given by  $\Delta\chi^2$ , of the  $a/b$  that minimize  $\chi^2$ . This provides an uncertainty estimate on  $a$  and  $b$ .

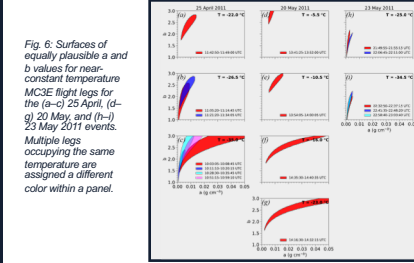


Fig. 6: Surfaces of equally plausible  $a$  and  $b$  values for near-constant temperature MC3E flight legs for the (a-c) 25 April, (d-g) 20 May, and (h-i) 23 May 2011 events. Multiple legs occupying the same temperature are assigned a different color within a panel.

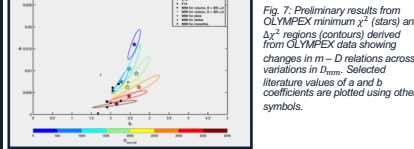


Fig. 7: Preliminary results from OLYMPEX minimum  $\chi^2$  (stars) and  $\Delta\chi^2$  regions (contours) derived from OLYMPEX data showing changes in  $m - D$  relations across variations in  $D_{mw}$ . Selected literature values of  $a$  and  $b$  coefficients are plotted using other symbols.

Results using MC3E (Fig. 6) and preliminary results using OLYMPEX flights (Fig. 7) indicate that there are coherent modes of  $a$  and  $b$  values that can be parameterized as a function of  $D_{mw}$  (a quantity that can be retrieved using remote sensing using Z and IWC. A technique similar to Finlon et al. (2018), and using Z and IWC, we find that values of a vary considerably (b less so in an absolute sense) as a function of observed  $D_{mw}$ , meaning that single mass-diameter relations for precipitating ice- and mixed-phase clouds, as are commonly used in models and retrievals, should not be expected able to capture observed mass-size variability due to the natural variation in hydrometeor properties (i.e., through aggregation). We view this as a breakthrough to significantly reduce uncertainties in forward computations in IWC and Z.